JACC: CARDIOVASCULAR IMAGING
VOL. 4, NO. 3, 2011

ISSN 1936-878X/$36.00
PUBLISHED BY ELSEVIER INC.
DOI:10.1016/j.jcmg.2010.12.006

iREVIEWS

STATE-OF-THE-ART PAPER

Cardiac PET: A Versatile, Quantitative Measurement Tool for Heart Failure Management

Henry Gewirtz, MD
Boston, Massachusetts

Current American Heart Association/American College of Cardiology practice guidelines classify congestive heart failure (CHF) in 4 stages (A, B, C, and D). This review focuses on state-of-the-art and future applications of quantitative positron emission tomography (PET) myocardial perfusion and metabolic imaging in the clinical evaluation and treatment of patients in all CHF stages. Basic physiological and metabolic principles related to the regulation of myocardial blood flow and metabolism at various stages of CHF are briefly reviewed. The advantages of quantitative PET image analysis in contrast to simple qualitative visual analysis of the scans also will be addressed. Finally, potential future clinical applications of quantitative PET for CHF evaluation and treatment will be discussed. (J Am Coll Cardiol Img 2011;4: 292–302) © 2011 by the American College of Cardiology Foundation

Current American Heart Association/American College of Cardiology guidelines recommend consideration of congestive heart failure (CHF) in 4 stages (A, B, C, and D; Fig. 1) (1). Stages A and B represent preclinical CHF (stage A: patient at high risk but without structural heart disease; stage B: structural heart disease present but symptoms/signs of CHF absent). Stages C and D reflect overt CHF (stage C: structural heart disease present with prior or current symptoms of CHF; stage D: refractory CHF requiring specialized intervention). The incidence of CHF in the United States has been increasing steadily in recent years (400,000 new cases every year estimated by the National Heart, Lung and Blood Institute in 1996), and mortality, particularly in stage D, is in excess of 50% per year (2). Accordingly, the syndrome represents a major public health problem. Ischemic heart disease (IHD) and hypertension are the most common causes of CHF, although obesity and diabetes, even in the absence of overt IHD but frequently present together and often with hypertension, are increasingly recognized as common etiologies (2). Quantitative positron emission tomography (PET) imaging plays an important role in both diagnosis of etiology and assessment of treatment of CHF at various stages of the syndrome and provides prognostic information as well. The current state of the art and future directions for quantitative PET imaging in CHF is the focus of this review, which will also address the advantages of the quantitative approach in contrast to simple qualitative visual interpretation of PET cardiac images.

From the Department of Medicine (Cardiology Division), Massachusetts General Hospital, Harvard Medical School, Boston, Massachusetts. Dr. Gewirtz has received a research grant from FluoroPharma, Inc.

Manuscript received November 9, 2010; revised manuscript received December 20, 2010, accepted December 23, 2010.

Quantitative PET Imaging in Patients With CHF: State of the Art

The role for state-of-the-art quantitative PET measurement of myocardial blood flow (MBF) (Fig. 2) and metabolism (glucose and fatty acid) depends on the specific clinical question(s) to be addressed. However, in more general terms, there are several points that should be made concerning the advantages of quantitative versus qualitative simple visual analysis of cardiac PET images in patients with CHF. First, simple visual analysis of PET myocardial perfusion images requires the assumption of a "normal" perfusion or metabolic zone—an erroneous assumption and clearly a major limitation of that approach. Second, simple visual interpretation is by definition subjective and hence liable to all associated shortcomings. Third, it has been shown in a modern clinical trial (PARR 2 [PET and Recovery Following Revascularization]) (3,4) and older observational studies (5–9) that objective measurement of parameters indicative of myocardial viability or myocardial flow reserve are valuable in improving patient management or assessing prognosis in patients with CHF. Such parameters (e.g., quantitative, objective determination and extent of MBF/^{18}F-fluorodeoxyglucose [FDG] "mismatch" and ^{82}Rb myocardial tracer kinetics and measurement of myocardial flow reserve) necessitate state-of-the-art quantitative PET imaging of MBF and metabolism and cannot be obtained by simple visual analysis of static PET images. Finally, potential future clinical applications for PET cardiac imaging in CHF (e.g., risk assessment for sudden cardiac death in patients with ischemic cardiomyopathy; PARAPET [Prediction of Arrhythmic Events With Positron Emission Tomography] trial) (10–13) will depend on adoption of current state-of-the-art quantitative PET methodologies used in such trials for assessment of MBF, glucose metabolism, and sympathetic nervous system function.

Pathophysiology of MBF and Clinical Applications of PET in Left Ventricular Dysfunction and CHF

Ischemic cardiomyopathy. Endothelial dysfunction related to dyslipidemia and oxidant stress (14,15) is known to affect the coronary microcirculation before the onset of overt coronary atherosclerosis and therefore places affected individuals in stage A CHF (high risk, without structural heart disease). Ongoing dyslipidemia, oxidant stress, and resulting endothelial dysfunction commonly progress to overt coronary atherosclerosis (stage B CHF), which in turn may be complicated by acute myocardial infarction and resulting left ventricular (LV) dysfunction or frank CHF (stage C CHF). Extensive myocardial damage from either a single or multiple infarcts may result in refractory CHF requiring specialized treatment or intervention (stage D CHF). Positron emission tomography measurements of absolute myocardial blood flow play an important role in patient management at each stage of CHF related to IHD or predisposing conditions such as obesity, hypertension, diabetes, dyslipidemia, and smoking. PET assessment of myocardial viability (typically with combined MBF and glucose [^{18}F-FDG] metabolism study) is especially important in stages C and D CHF.

The role of PET measurements of MBF in assessment of coronary microvascular function has been reviewed extensively (14–16). Even asymptomatic patients with dyslipidemia without manifest IHD may have abnormal myocardial flow reserve owing to coronary microvascular dysfunction (17). The same is true of patients with obesity, diabetes, and hypertension either alone or in combination (18). A common mechanism in each of these conditions is endothelial dysfunction related to oxidant stress and subsequent reduction in nitric oxide bioavailability (18–21). Depending on whether or not LV hypertrophy is present in association with hypertension, mechanical compressive forces and interstitial fibrosis also may play a role (22). Circulating vasoactive peptides (e.g., endothelin) (23) also may contribute to impairment of coronary microvascular dilator capacity. Finally, it has been shown that evidence of increased serum levels of circulating biomarkers of inflammation increase the risk of developing CHF (24–26) and may do so at least in part via the oxidant stress mechanism noted earlier.

ABBREVIATIONS AND ACRONYMS

CAV = coronary artery vasculopathy
CHF = congestive heart failure
DCM = dilated cardiomyopathy
FDG = fluorodeoxyglucose
FFA = free fatty acid
IHD = ischemic heart disease
IVUS = intravascular ultrasound
LV = left ventricular
MBF = myocardial blood flow
PET = positron emission tomography

Several small observational studies in humans have suggested that PET measurements of absolute MBF and MBF reserve may be useful in providing prognostic information concerning progression from stage A/B to C/D CHF in patients with hypertrophic (5,27) or idiopathic dilated cardiomyopathy (DCM) (7). Although the studies have certain limitations in addition to small sample size, such as reliance on flow reserve ratio as an end point, they nevertheless demonstrated the potential for quantitative measurements of absolute MBF to

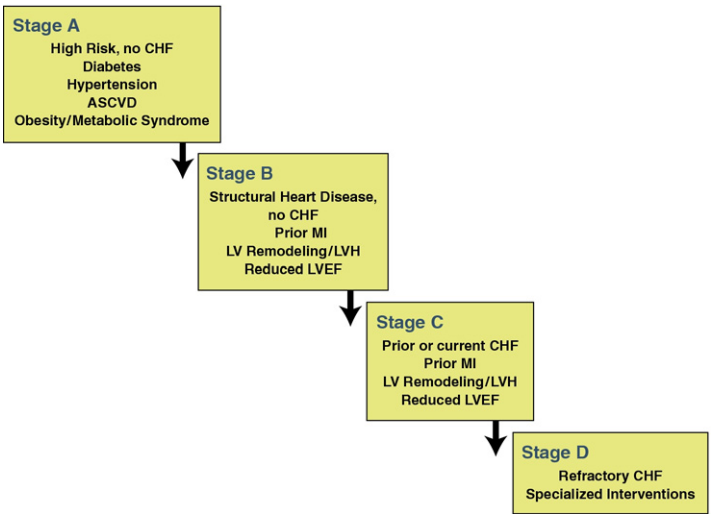

Figure 1. American Heart Association/American College of Cardiology Guideline for Clinical Staging of CHF

ASCVD = atherosclerotic cardiovascular disease; CHF = congestive heart failure; LV = left ventricular; LVEF = left ventricular ejection fraction; LVH = left ventricular hypertrophy; MI = myocardial infarction.

provide important clinical information unavailable from simple qualitative visual analysis of the images. Similar data regarding prognosis have been reported for patients with IHD (28). More widespread application of clinical insights derived from these studies is now possible with generator-derived ^{82}Rb for PET measurements of absolute MBF and MBF reserve with a commercially available Food and Drug Administration–approved computer program (Corridor 4DM, CFR option, INVIA Medical Imaging Solutions, Ann Arbor, Michigan). The program has been validated by comparison with ^{13}N-ammonia measurements of MBF in humans (29) and therefore is suitable for use with ^{13}N-ammonia as well. As noted earlier, use of quantitative measurements of MBF do not depend on the invalid assumption of an obligatory "normal" zone and so are inherently superior to simple qualitative visual assessment of these images. Further, as ^{18}F-labeled MBF tracers (e.g., ^{18}F-BMS-747158-02 [30] and possibly ^{18}F-BFPET [31]) become available, the ability to make these measurements will become even more widespread. In addition to providing prognostic information, which may be helpful in guiding CHF management at an early stage, quantitative PET measurements of MBF will permit establishment of baseline pre-treatment levels of maximal MBF and therefore provide an objective parameter for subsequent follow-up exams designed to assess the effects of therapy (e.g., statins [32]) in patients judged to be at high risk for progression to more advanced stages (C and D) of CHF.

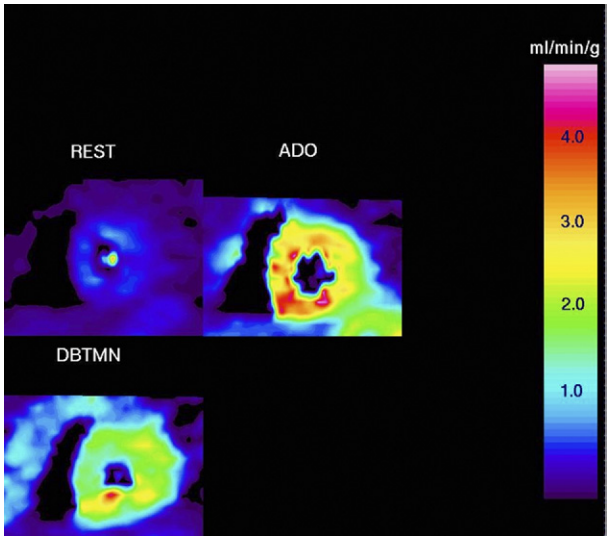

Figure 2. Parametric ^{13}N-Ammonia Myocardial Blood Flow Images

The color scale (ml/min/g) is shown at the right for rest, adenosine (ADO), and dobutamine (DBTMN) conditions in a healthy human subject.

The use of PET quantitative assessment of absolute MBF and myocardial glucose metabolism is more clearly established in the setting of stages C and D CHF. When signs and symptoms of CHF are first manifest but the etiology has not been established, it is common practice to perform diagnostic cardiac catheterization and coronary angiography. However, PET quantitative assessment of

absolute MBF will be very helpful in a variety of settings. Patients with chronic renal insufficiency, not yet on dialysis, are at high risk for severe worsening of renal function with coronary angiography. PET quantitative assessment of absolute MBF with ^{13}N-ammonia or ^{82}Rb is an excellent method for assessment of the coronary circulation in such cases. Detection of hemodynamically significant stenoses in each of the 3 major coronary vascular territories is possible with a single MBF measurement obtained during adenosine infusion (33). The same methodology also should be considered for patients whose prior probability for IHD is low (<10%) and certainly for those with coronary stenoses of uncertain physiological significance (see the following paragraph and Figure 3).

PET quantitative assessment of absolute MBF during adenosine stress may be thought of as a noninvasive fractional flow reserve test (33) (Fig. 3). In this regard, it should be noted that coronary intervention(s) performed in patients with abnormal fractional flow reserve were associated in the FAME (Fractional Flow Reserve Versus Angiography for Multivessel Evaluation) trial (34) with reduced rates of the primary end point at 1 year (death, nonfatal myocardial infarction, and repeat revascularization) compared with that of similar patients in whom percutaneous coronary interventions were performed based on visual assessment of the lesions alone. This study thus provided another example of the superiority of objective physiological assessment over simple qualitative visual inspection of images in the evaluation and treatment of patients with IHD. Moreover, acquiring an electrocardiogram-gated image of the myocardium following completion of the dynamic acquisition for MBF measurements makes it possible to assess LV function, including LV volumes, LV ejection fraction, and stroke work and power (35–37). These measurements of LV contractile function not only are useful in following the response to therapy but also are essential to the proper interpretation of absolute measurements of MBF in the case of stroke work and power.

PET measurements of absolute MBF also have been employed in the past to help elucidate the pathophysiology of myocardial hibernation and stunning (38–44), which are frequently present in stages C and D CHF. Although it is clear that a chronic state characterized by matched reduction of MBF and contractile function (hibernation) exists in humans (41), chronic stunning (relatively preserved MBF with impaired contraction) also is known to occur (44), sometimes in the same patients (41), and may progress to chronic hibernation (42). These states are of considerable importance in the clinical evaluation of patients with IHD with stages C and especially D CHF. In particular, efforts to detect myocardial viability in one or more coronary vascular territories frequently play a key role in clinical decision making regarding revascularization.

The established PET method for assessment of myocardial viability compares the uptake of ^{18}F-

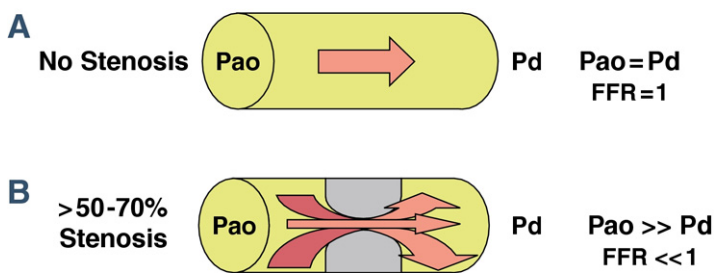

Figure 3. Schematic Representation of the Physiological Basis for FFR Measurement

The pressure drop (dP) across a coronary stenosis is given by the equation dP = aQ + bQ2, for which a and b are constants related to stenosis geometry and blood viscosity (80–82). Under conditions in which there is no stenosis **(A)**, the value of each constant approaches 0, and so there is no dP along the epicardial vessel during adenosine infusion. Accordingly, the fractional flow reserve (FFR) is approximately 1 (mean aortic pressure [Pao] = mean pressure distal to the stenosis [Pd]). With increasing stenosis severity, the values of a and b increase and, more importantly, flow accelerates across the narrowed vessel lumen **(B)** such that there is a geometric pressure loss (note the term bQ2), with resulting decline in Pd. Thus, FFR becomes much less than 1 because Pao >> Pd. Q = myocardial blood flow.

FDG with that of rest MBF (9), as represented by static PET ^{13}N-ammonia or ^{82}Rb uptake images. Regions with ^{18}F-FDG uptake in excess of MBF ("mismatch") generally are viable and have been shown to improve contraction following revascularization (6,9,41). It is important to note that the original description of the observation (9) and recent clinical trials (4,45) used quantitative normalized measurement of tracer concentration and standardized definitions to determine the presence and extent of ^{18}F-FDG MBF "mismatch." Simple qualitative visual assessment was not used. Moreover, the extent of FDG/blood flow "mismatch," objectively measured, has been shown both to have prognostic information and to be helpful in decision making regarding coronary revascularization in ischemic cardiomyopathy (3,4,6). Such information is not available from simple visual analysis of the images. Accordingly, to obtain optimal results, especially to define the extent of "mismatch" territory, state-of-the-art clinical practice should apply methods shown to be of value in prior clinical trials. Although, in theory, Patlak analysis to determine the metabolic rate for glucose usage combined with absolute measurement of MBF should be superior to the quantitative normalized method for determining viability precisely because it avoids the assumption of an obligatory "normal" zone (typically that with the best ^{13}N-ammonia or ^{82}Rb uptake), this approach has not been reported and remains a direction for future research.

PET measurements of absolute MBF alone in this setting are predictive of myocardial scar at very low flows, <0.3 ml/min/g, which commonly correspond to regions of poor ^{18}F-FDG uptake (38,46,47). However, at higher levels of rest MBF, overlap between viable and nonviable regions precludes exclusive use of absolute MBF for viability assessment (Fig. 4). Nevertheless, quantitative measurements of PET ^{82}Rb washout (8) or ^{13}N-ammonia tracer kinetic parameters (e.g., K1/k2 [46] and k3 [47]), which cannot be obtained from simple visual analysis of uptake images, have been shown to enhance detection of viable myocardium in patients with ischemic cardiomyopathy and in conjunction with absolute measurement of MBF suggest a potential future alternative to ^{18}F-FDG MBF "mismatch" for viability assessment.

Another PET method, measurement of myocardial oxygen consumption with ^{11}C-acetate, has been used to assess myocardial viability and was shown to be superior to that of ^{18}F-FDG in one lab (48). The method is limited, however, by the need

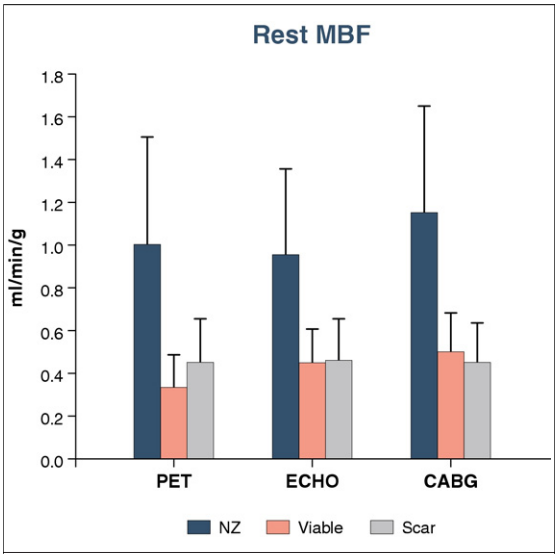

Figure 4. Group Mean (+ SD) Data Depicting the Relationship Between Rest MBF and Myocardial Viability as Defined by PET, ECHO, and Contractile Response to CABG Criteria

By all 3 methods, regions of chronically reduced myocardial blood flow (MBF) corresponded to viable myocardial segments. In the MBF range of > 0.3 ml/min/g, there is considerable overlap between viable and nonviable segments. Reprinted, with permission, from Tawakol et al. (41). CABG = coronary artery bypass graft; ECHO = echocardiography; NZ = normal zone; PET = positron emission tomography.

for an on-site cyclotron to produce the tracer and therefore has not gained widespread acceptance. Finally, it should be noted that cardiac magnetic resonance (CMR), with gadolinium contrast and pulse sequence designed to optimize delayed (5 to 20 min post–contrast injection) hyperenhancement of scar tissue (49), has been found to be an accurate method for assessment of myocardial viability, compares quite favorably with PET ^{18}F-FDG methodology (50), and is becoming increasingly used for this purpose.

Other potential applications for PET measurements of absolute MBF that have not yet achieved wide clinical application but are pertinent, particularly to stage D CHF, often but not always of ischemic origin, include baseline and follow-up measurements in patients after cardiac transplant (51–54) and those with LV assist device support (55) or cardiac resynchronization therapy with biventricular pacemaker (56). Follow-up of patients after cardiac transplantation represents perhaps the most useful of these potential applications, given the importance of post-transplant coronary artery vasculopathy (CAV) in determining the clinical course of these patients (57). Coronary angiography, coronary intravascular ultrasound (IVUS), or

both are routinely employed annually to detect anatomic evidence of epicardial coronary stenoses or diffuse intimal thickening of varying degree related to CAV (57–59). Both methods are invasive and provide anatomic as opposed to functional information concerning the status of coronary circulation. Moreover, because of diffuse intimal thickening, the epicardial coronary vessels may appear angiographically normal (58,59), whereas disease primarily involving very small intramyocardial vessels including the microcirculation (51,60) cannot be visualized by routine angiography or IVUS.

Because the vasodilator capacity of the coronary microcirculation changes as a function of time post-transplant even in the absence of epicardial stenoses (51), it is important in interpreting PET measurements of absolute MBF (rest and with adenosine or other direct coronary vasodilator) to be cognizant of the duration post-transplant at the time of measurement (Fig. 5). In the first year post-transplant, rest MBF may be elevated relative to demand, although dilator capacity is normal (vs. healthy controls) (51). Between 1 and 3 years post-transplant, both rest MBF and maximal dilator capacity typically are normal. However, after 3 years, microvascular dilator capacity declines versus normal (51). A rough inverse correlation between extent of intimal thickening by IVUS (plaque volume) and myocardial flow reserve assessed by PET ^{13}N-ammonia recently has been reported (52). The loose inverse relationship clearly illustrates the well-known problem of comparing anatomic with physiological measurements and, more importantly, raises the question of which is better for assessment of prognosis and evaluation of therapy aimed at preventing or at least ameliorating CAV. Although the answer is not known, it appears likely that the functional measurements (i.e., absolute MBF) may prove superior because in the case of coronary microcirculation, abnormal vasodilator capacity related to abnormal endothelial function precedes recognizable structural abnormalities.

Stem cell and gene therapy to treat stages C and D CHF, particularly that related to IHD, is an active research area. Whereas studies with positron-emitting reporter probes (61) have sought to document the presence, location, and fate of engrafted cells or gene expression, functional studies of the coronary circulation in such patients have been limited and involved standard single-photon emission computed tomography myocardial perfusion imaging (62). However, a recent PET study of

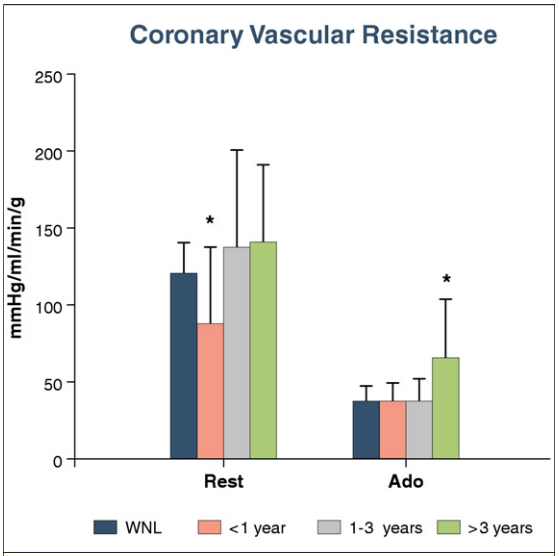

Figure 5. Group Mean (+ SD) Data Depicting the Time Course of Changes in Rest and Minimal (Adenosine) CVR Following Cardiac Transplantation in Humans With Normal Coronary Angiograms

Note that in the early post-transplant period, rest coronary vascular resistance (CVR) is reduced versus both normal controls (WNL) and other transplant groups (<1 year, 1–3 years, and >3 years). More than 3 years following cardiac transplantation, there is evidence of progressive microvascular dysfunction with a significant increase in minimal CVR. *$p < 0.05$ versus other groups. Reprinted, with permission, from Kushwaha et al. (51). Ado = adenosine; WNL = within normal limits.

MBF reserve in patients treated with vascular endothelial growth factor has been reported (63). Given that the placebo effect is known to complicate interpretation of these studies, objective methods to document improvement are essential not only in the research setting but also for subsequent clinical management. Indeed, a recent pilot study employed both quantitative PET measurements of MBF (^{13}N-ammonia) and ^{18}F-FDG for glucose metabolism to define viability by objective criteria and obtain gated ^{18}F-FDG images for objective measurement of LV function in patients treated with bone marrow–derived stem cells following myocardial infarction (64). Although preliminary, quantitative PET data identified a subset of patients in whom stem cell therapy appeared to reduce scar size and improve rest MBF and LV function. The study is illustrative of the role and future direction for state-of-the-art quantitative PET measurements of MBF and metabolism in assessment of the efficacy of state-of-the-art therapy for stages C and D CHF.

Nonischemic cardiomyopathy. Obesity, diabetes, and hypertension commonly coexist in a given patient and either alone or in combination may result in

DCM absent atherosclerotic coronary artery disease. In addition to important coronary microvascular dysfunction in these patients (14,15), abnormalities in both glucose and fatty acid metabolism are known to occur and have been reviewed in detail recently (65–69). Although beta oxidation of free fatty acids (FFA) is the principal source of ATP production by cardiomyocyte mitochondria under resting conditions in the normal heart, it is important to recall that glucose also is used and that the substrate utilization will vary depending on the metabolic milieu and physiological conditions (65,67). Thus, with exercise, glucose usage increases relative to FFA beta oxidation. Moreover, it has been pointed out from a metabolic view that the heart does best when using an appropriate mix of carbohydrate and FFA as fuels (Fig. 6) and that excessive shift to either glucose or FFA metabolism may result in cardiotoxicity (67,68).

Diabetes has been noted to be an important example in which insulin resistance leads to excessive use of FFA by the myocardium, with resulting lipotoxicity (68,69). Under such conditions, the heart's ability to oxidize FFA (and glucose) is impaired, and consequently ATP production declines, with the result that the heart behaves as "if starved in the midst of plenty" (66–69). Lipotoxicity is associated with a number of other maladaptive processes including accumulation of triglycerides, reactive oxidant species, and activators of various genetic transcription factors (68,69). In addition, excessive FFA metabolism inhibits glucose oxidation and results in accumulation of intermediary products of glycolysis. These products are potentially cardiotoxic and may active genetic pathways, particularly fetal programs, that may become maladaptive (70), and together result in what has been termed glucolipotoxicity (69,71). Finally, it has been reported that more advanced stages of CHF (C and D) may themselves cause myocardial insulin resistance and therefore result in a vicious cycle in which CHF impairs intermediate energy metabolism, which in turn exacerbates CHF (70,72).

Currently, there is great research potential for PET imaging of cardiac metabolic pathways and gene programs involved in the basic mechanisms underlying CHF of ischemic and nonischemic etiologies at all stages (66,73). Clinical applications, unfortunately, are limited by a number of factors, including requirement for an on-site cyclotron and radiochemist to manufacture ^{11}C-labeled metabolic intermediates and complexity of the studies that range from patient dietary preparation to advanced tracer kinetic models needed for quantitative results. It may be possible in the future to minimize many of these issues with a previously reported ^{18}F-labeled fatty acid tracer (74).

One quantitative study with ^{18}F-FDG in humans under conditions of a hyperinsulinemic, euglycemic clamp demonstrated that young patients with insulin-dependent diabetes of <5 years' duration had similar insulin-stimulated myocardial glucose uptake compared with healthy controls (75). Further, given current interest in cardiac metabolism as a target for CHF therapy at various stages (67,70,76), the ability to quantitatively measure glucose use with ^{18}F-FDG in humans (Fig. 7) under well-defined metabolic and hemodynamic conditions may prove helpful in determining if a particular therapy (drug or device) enhances myocardial glucose usage, which is more efficient in comparison with FFA beta oxidation in terms of oxygen consumption for production of ATP (70). Moreover, the ability to gate the FDG acquisition permits near simultaneous assessment of LV contractile function (64,77) and therefore provides direct information on the therapeutic efficacy of the metabolic intervention. Accordingly, quantitative PET

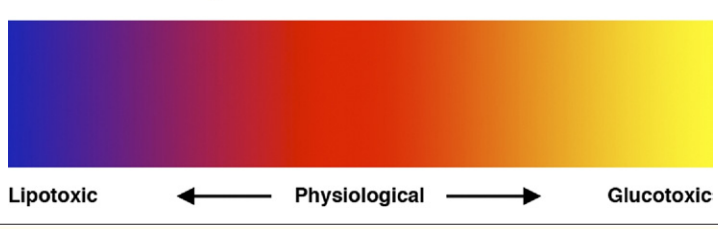

Figure 6. Schematic Representation of Myocardial Use of FA and CHO in the Human Heart

Under physiological conditions, the myocardium employs a mixture of fatty acids (FA) and carbohydrates (CHO) to fuel energy production. Excessive reliance on one or the other is maladaptive and leads to lipotoxicity (FA), glucotoxicity (CHO), or a combined state known as glucolipotoxicity (69).

measurements of cardiac glucose metabolism and contractile function are readily available in the clinical setting and are likely to play a more important role in patient management as metabolic interventions become more widely applied and the need to demonstrate efficacy increases in a socioeconomic environment that demands the optimal use of scarce health care resources.

Further, it may be anticipated that the advent of ^{18}F-labeled fatty acid and sympathetic nerve (78) tracers will substantially expand the field of cardiac metabolic and autonomic nervous system imaging for clinical use in patients with CHF, especially when combined with quantitative measurements of glucose metabolism, LV function. and MBF. Lastly, quantitative PET imaging of ^{18}F-FDG in humans has been reported useful in distinguishing idiopathic DCM from that owing to isolated cardiac sarcoidosis and for assessing both disease activity and response to therapy (79). The quantitative methodology employed required determination of standard uptake values of ^{18}F-FDG in a standard 17-segment model, along with means, SDs, and coefficients of variation, all of which are not possible with simple qualitative visual analysis. The last parameter (coefficients of variation) was essential to objectively defining "heterogeneous" tracer uptake and best separated patients with cardiac sarcoidosis from those with DCM, as well as controls and patients with sarcoidosis but without cardiac involvement.

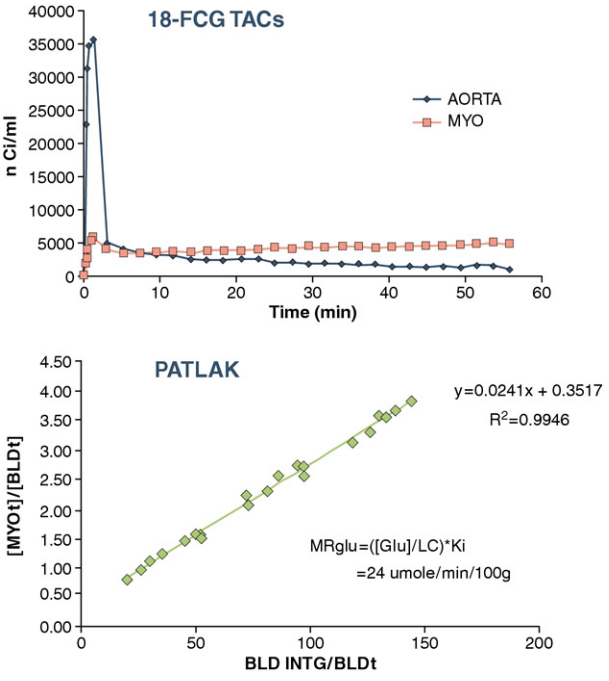

Figure 7. Typical LV Blood Pool and Myocardial TAC From PET ^{18}F-FDG Dynamic Data Acquisition

Shown here are typical LV blood pool and myocardial time activity curves (TAC) (**upper panel**) from a PET ^{18}F-fluorodeoxyglucose (FDG) dynamic data acquisition. The **lower panel** shows the resulting Patlak plot for the data. The slope of the line, Ki, is the uptake rate constant for the tracer and when multiplied by measured plasma glucose concentration divided by the lumped constant (LC) gives the metabolic rate for glucose usage (mGLU) (μmol/min/100 g). Note that the plot can be implemented with an ordinary spreadsheet, and the LC is not constant over all physiological conditions; a method for correcting it based on the myocardial FDG TAC has been proposed (83). Other abbreviations as in Figures 1 and 4.

Conclusions

PET quantitative measurements of MBF and metabolism provide state-of-the-art methodology for evaluation and management of patients at all stages of CHF. In stages A and B, quantitative measurements of absolute MBF permits assessment of coronary microvascular function, which are impossible to obtain with simple visual analysis of uptake images and which have been shown to provide prognostic information (5,7) and information on response to therapy (32). In the more advanced stages of CHF (C and D), quantitative PET measurements of MBF and glucose metabolism are of proven value in assessment of myocardial viability (4,9,45), prognosis (6), and selection of patients for coronary revascularization (3). Applications that are immediately and readily available but not yet widely employed include absolute measurement of MBF for detection of CAV (51), a key prognostic factor, in patients with cardiac transplants; quantitative measurement of the metabolic rate for glucose usage and LV function for assessment of response to metabolic therapy of stages C and D CHF; objective treatment responses to device, gene, or stem cell therapy (64), as defined by absolute MBF, quantitative glucose metabolism, and LV function; and quantitative ^{18}F-FDG uptake to improve the diagnosis of at least one treatable cause of cardiomyopathy, sarcoidosis (79). Finally, it is important to emphasize that: 1) quantitative measurements of MBF in the stenosis setting are linked to basic fluid dynamic principles (80–82) which are the basis for the invasive fractional flow reserve measurement; and 2) quantitative measurements of the metabolic rate for glucose usage depend on the value assigned to the "lumped constant" which in fact is not constant and requires correction depending on physiological condition (83).

Future applications will depend on availability of ^{18}F-labeled tracers for widespread use and include

JACC: CARDIOVASCULAR IMAGING, VOL. 4, NO. 3, 2011
MARCH 2011:292–302

assessment of myocardial fatty acid metabolism and autonomic nervous system function, both of which are important clinically with respect to risk stratification and evaluation of innovative, emerging therapies for CHF. As illustrated earlier, optimal use of PET for these applications will require state-of-the-art quantitative methods to provide objective, measureable parameters that can be accurately reproduced, automated, and followed over time, and are independent of and inherently superior to even a skilled reader's subjective impression of a static PET image.

Reprint requests and correspondence: Dr. Henry Gewirtz, Cardiac Unit/Yawkey 5E, Massachusetts General Hospital, Boston, Massachusetts 02114. *E-mail: hgewirtz@partners.org.*

REFERENCES

1. Jessup M, Abraham WT, Casey DE, et al. 2009 focused update: ACCF/AHA guidelines for the diagnosis and management of heart failure in adults: a report of the American College of Cardiology Foundation/American Heart Association Task Force on Practice Guidelines: developed in collaboration with the International Society for Heart and Lung Transplantation. J Am Coll Cardiol 2009;53:1343–82.
2. Kannel WB. Incidence and epidemiology of heart failure. Heart Fail Rev 2000;5:167–73.
3. Abraham A, Nichol G, Williams KA, et al. ^{18}F-FDG PET imaging of myocardial viability in an experienced center with access to ^{18}F-FDG and integration with clinical management teams: the Ottawa-FIVE substudy of the PARR 2 trial. J Nucl Med 2010;51:567–74.
4. Beanlands RS, Nichol G, Huszti E, et al. F-18-fluorodeoxyglucose positron emission tomography imaging-assisted management of patients with severe left ventricular dysfunction and suspected coronary disease: a randomized, controlled trial (PARR-2). J Am Coll Cardiol 2007;50:2002–12.
5. Cecchi F, Olivotto I, Gistri R, et al. Coronary microvascular dysfunction and prognosis in hypertrophic cardiomyopathy. N Engl J Med 2003;349:1027–35.
6. Maddahi J, Schelbert H, Brunken R, Di Carli M. Role of thallium-201 and PET imaging in evaluation of myocardial viability and management of patients with coronary artery disease and left ventricular dysfunction. J Nucl Med 1994;35:707–15.
7. Neglia D, Michelassi C, Trivieri MG, et al. Prognostic role of myocardial blood flow impairment in idiopathic left ventricular dysfunction. Circulation 2002;105:186–93.
8. vom Dahl J, Muzik O, Wolfe ER Jr., et al. Myocardial rubidium-82 tissue kinetics assessed by dynamic positron emission tomography as a marker of myocardial cell membrane integrity and viability. Circulation 1996;93:238–45.
9. Tillisch J, Brunken R, Marshall R, et al. Reversibility of cardiac wall-motion abnormalities predicted by positron tomography. N Engl J Med 1986;314:884–8.
10. Fallavollita JA, Banas MD, Suzuki G, et al. ^{11}C-meta-hydroxyephedrine defects persist despite functional improvement in hibernating myocardium. J Nucl Cardiol 2010;17:85–96.
11. Fallavollita JA, Canty JM Jr. Dysinnervated but viable myocardium in ischemic heart disease. J Nucl Cardiol 2010;17:1107–15.
12. Fallavollita JA, Luisi AJ Jr., Michalek SM, et al. Prediction of arrhythmic events with positron emission tomography: PAREPET study design and methods. Contemp Clin Trials 2006;27:374–88.
13. Fallavollita JA, Luisi AJ Jr., Yun E, deKemp RA, Canty JM Jr. An abbreviated hyperinsulinemic-euglycemic clamp results in similar myocardial glucose utilization in both diabetic and non-diabetic patients with ischemic cardiomyopathy. J Nucl Cardiol 2010;17:637–45.
14. Camici PG, Crea F. Coronary microvascular dysfunction. N Engl J Med 2007;356:830–40.
15. Schindler TH, Schelbert HR, Quercioli A, Dilsizian V. Cardiac PET imaging for the detection and monitoring of coronary artery disease and microvascular health. J Am Coll Cardiol Img 2010;3:623–40.
16. Gould KL. Does coronary flow trump coronary anatomy? J Am Coll Cardiol Img 2009;2:1009–23.
17. Dayanikli F, Grambow D, Muzik O, et al. Early detection of abnormal coronary flow reserve in asymptomatic men at high risk for coronary artery disease using positron emission tomography. Circulation 1994;90:808–17.
18. Levy BI, Schiffrin EL, Mourad JJ, et al. Impaired tissue perfusion: a pathology common to hypertension, obesity, and diabetes mellitus. Circulation 2008;118:968–76.
19. Loscalzo J. Oxidant stress: a key determinant of atherothrombosis. Biochem Soc Trans 2003;31(Pt 5):1059–61.
20. Quyyumi AA, Dakak N, Andrews NP, et al. Contribution of nitric oxide to metabolic coronary vasodilation in the human heart. Circulation 1995;92:320–6.
21. Treasure C, Klein L, Vita J, et al. Hypertension and left ventricular hypertrophy are associated with impaired endothelium—mediated relaxation in human coronary resistance vessels. Circulation 1993;87:86–93.
22. Hamasaki S, Al Suwaidi J, Higano ST, et al. Attenuated coronary flow reserve and vascular remodeling in patients with hypertension and left ventricular hypertrophy. J Am Coll Cardiol 2000;35:1654–60.
23. Parris R, Webb D. The endothelin system in cardiovascular physiology and pathophysiology. Vasc Med 1997;2:31–43.
24. Suzuki T, Katz R, Jenny NS, et al. Metabolic syndrome, inflammation, and incident heart failure in the elderly: the cardiovascular health study. Circ Heart Fail 2008;1:242–8.
25. Suzuki T, Hirata K, Elkind MS, et al. Metabolic syndrome, endothelial dysfunction, and risk of cardiovascular events: the Northern Manhattan Study (NOMAS). Am Heart J 2008;156:405–10.
26. Bahrami H, Bluemke DA, Kronmal R, et al. Novel metabolic risk factors for incident heart failure and their relationship with obesity: the MESA (Multi-Ethnic Study of Atherosclerosis) study. J Am Coll Cardiol 2008;51:1775–83.
27. Olivotto I, Cecchi F, Gistri R, et al. Relevance of coronary microvascular flow impairment to long-term remodeling and systolic dysfunction in hypertrophic cardiomyopathy. J Am Coll Cardiol 2006;47:1043–8.
28. Herzog BA, Husmann L, Valenta I, et al. Long-term prognostic value of ^{13}N-ammonia myocardial perfusion positron emission tomography added value of coronary flow reserve. J Am Coll Cardiol 2009;54:150–6.

29. El Fakhri G, Kardan A, Sitek A, et al. Reproducibility and accuracy of quantitative myocardial blood flow assessment with ^{82}Rb PET: comparison with ^{13}N-ammonia PET. J Nucl Med 2009;50:1062–71.
30. Nekolla SG, Reder S, Saraste A, et al. Evaluation of the novel myocardial perfusion positron-emission tomography tracer ^{18}F-BMS-747158-02: comparison to ^{13}N-ammonia and validation with microspheres in a pig model. Circulation 2009;119:2333–42.
31. Shoup TM, Elmaleh DR, Brownell AL, et al. Evaluation of (4-[^{18}F]fluorophenyl)triphenylphosphonium ion. A potential myocardial blood flow agent for PET. Mol Imaging Biol 2010 Jun 19 [Epub ahead of print].
32. Huggins GS, Pasternak RC, Alpert NM, Fischman AJ, Gewirtz H. Effects of short-term treatment of hyperlipidemia on coronary vasodilator function and myocardial perfusion in regions having substantial impairment of baseline dilator reverse. Circulation 1998;98:1291–6.
33. Hajjiri MM, Leavitt MB, Zheng H, et al. Comparison of positron emission tomography measurement of adenosine-stimulated absolute myocardial blood flow versus relative myocardial tracer content for physiological assessment of coronary artery stenosis severity and location. J Am Coll Cardiol Img 2009;2:751–8.
34. Tonino PA, De Bruyne B, Pijls NH, et al. Fractional flow reserve versus angiography for guiding percutaneous coronary intervention. N Engl J Med 2009;360:213–24.
35. Porenta G, Cherry S, Czernin J, et al. Noninvasive determination of myocardial blood flow, oxygen consumption and efficiency in normal humans by carbon-11 acetate positron emission tomography imaging. Eur J Nucl Med 1999;26:1465–74.
36. Khorsand A, Graf S, Eidherr H, et al. Gated cardiac ^{13}N-NH_3 PET for assessment of left ventricular volumes, mass, and ejection fraction: comparison with electrocardiography-gated ^{18}F-FDG PET. J Nucl Med 2005;46:2009–13.
37. Gregory SA, MacRae CA, Aziz K, et al. Myocardial blood flow and oxygen consumption in patients with Friedreich's ataxia prior to the onset of cardiomyopathy. Coron Artery Dis 2007;18:15–22.
38. Gewirtz H, Fischman AJ, Abraham SA, et al. Positron emission tomographic measurements of absolute regional myocardial blood flow permits identification of nonviable myocardium in patients with chronic myocardial infarction. J Am Coll Cardiol 1994;23:851–9.
39. Berman M, Fischman AJ, Southern J, et al. Myocardial adaptation during and after sustained, demand-induced ischemia. Observations in closed-chest, domestic swine. Circulation 1996;94:755–62.
40. Holmvang G, Fry S, Skopicki HA, et al. Relation between coronary "steal" and contractile function at rest in collateral-dependent myocardium of humans with ischemic heart disease. Circulation 1999;99:2510–6.
41. Tawakol A, Skopicki HA, Abraham SA, et al. Evidence of reduced resting blood flow in viable myocardial regions with chronic asynergy. J Am Coll Cardiol 2000;36:2146–53.
42. Heusch G, Schulz R, Rahimtoola SH. Myocardial hibernation: a delicate balance. Am J Physiol Heart Circ Physiol 2005;288:H984–99.
43. Fallavollita J, Canty JJ. Differential 18-F-2-deoxyglucose uptake in viable dysfunctional myocardium with normal resting perfusion: evidence for chronic stunning in pigs. Circulation 1999;99:2798–805.
44. Gerber BL, Vanoverschelde JJ, Bol A, et al. Myocardial blood flow, glucose uptake, and recruitment of inotropic reserve in chronic left ventricular dysfunction. Implications for the pathophysiology of chronic myocardial hibernation. Circulation 1996;94:651–9.
45. Beanlands RS, Ruddy TD, deKemp RA, et al. Positron emission tomography and recovery following revascularization (PARR-1): the importance of scar and the development of a prediction rule for the degree of recovery of left ventricular function. J Am Coll Cardiol 2002;40:1735–43.
46. Beanlands RS, deKemp R, Scheffel A, et al. Can nitrogen-13 ammonia kinetic modeling define myocardial viability independent of fluorine-18 fluorodeoxyglucose? J Am Coll Cardiol 1997;29:537–43.
47. Kitsiou AN, Bacharach SL, Bartlett ML, et al. ^{13}N-ammonia myocardial blood flow and uptake: relation to functional outcome of asynergic regions after revascularization. J Am Coll Cardiol 1999;33:678–86.
48. Gropler RJ, Geltman EM, Sampathkumaran K, et al. Comparison of carbon-11-acetate with fluorine-18-fluorodeoxyglucose for delineating viable myocardium by positron emission tomography. J Am Coll Cardiol 1993;22:1587–97.
49. Simonetti OP, Kim RJ, Fieno DS, et al. An improved MR imaging technique for the visualization of myocardial infarction. Radiology 2001;218:215–23.
50. Kuhl HP, Beek AM, van der Weerdt AP, et al. Myocardial viability in chronic ischemic heart disease: comparison of contrast-enhanced magnetic resonance imaging with ^{18}F-fluorodeoxyglucose positron emission tomography. J Am Coll Cardiol 2003;41:1341–8.
51. Kushwaha SS, Narula J, Narula N, et al. Pattern of changes over time in myocardial blood flow and microvascular dilator capacity in patients with normally functioning cardiac allografts. Am J Cardiol 1998;82:1377–81.
52. Wu YW, Chen YH, Wang SS, et al. PET assessment of myocardial perfusion reserve inversely correlates with intravascular ultrasound findings in angiographically normal cardiac transplant recipients. J Nucl Med 2010;51:906–12.
53. Preumont N, Berkenboom G, Vachiery J, et al. Early alterations of myocardial blood flow reserve in heart transplant recipients with angiographically normal coronary arteries. J Heart Lung Transplant 2000;19:538–45.
54. Preumont N, Lenaers A, Goldman S, et al. Coronary vasomotility and myocardial blood flow early after heart transplantation. Am J Cardiol 1996;78:550–4.
55. Xydas S, Rosen RS, Pinney S, et al. Reduced myocardial blood flow during left ventricular assist device support: a possible cause of premature bypass graft closure. J Heart Lung Transplant 2005;24:1976–9.
56. Knaapen P, van Campen LM, de Cock CC, et al. Effects of cardiac resynchronization therapy on myocardial perfusion reserve. Circulation 2004;110:646–51.
57. Konig A, Kilian E, Rieber J, et al. Assessment of early atherosclerosis in de novo heart transplant recipients: analysis with intravascular ultrasound-derived radiofrequency analysis. J Heart Lung Transplant 2008;27:26–30.
58. St. Goar FG, Pinto FJ, Alderman EL, et al. Intracoronary ultrasound in cardiac transplant recipients. In vivo evidence of "angiographically silent" intimal thickening. Circulation 1992;85:979–87.
59. Johnson DE, Alderman EL, Schroeder JS, et al. Transplant coronary artery disease: histopathologic correlations with angiographic morphology. J Am Coll Cardiol 1991;17:449–57.
60. Treasure CB, Vita JA, Ganz P, et al. Loss of the coronary microvascular response to acetylcholine in cardiac transplant patients. Circulation 1992;86:1156–64.

61. Inubushi M, Tamaki N. Positron emission tomography reporter gene imaging in the myocardium: for monitoring of angiogenic gene therapy in ischemic heart disease. J Card Surg 2005;20:S20–4.
62. Hendel RC, Henry TD, Rocha-Singh K, et al. Effect of intracoronary recombinant human vascular endothelial growth factor on myocardial perfusion: evidence for a dose-dependent effect. Circulation 2000;101:118–21.
63. Tio RA, Tan ES, Jessurun GA, et al. PET for evaluation of differential myocardial perfusion dynamics after VEGF gene therapy and laser therapy in end-stage coronary artery disease. J Nucl Med 2004;45:1437–43.
64. Castellani M, Colombo A, Giordano R, et al. The role of PET with ^{13}N-ammonia and ^{18}F-FDG in the assessment of myocardial perfusion and metabolism in patients with recent AMI and intracoronary stem cell injection. J Nucl Med 2010;51:1908–16.
65. Taegtmeyer H. Switching metabolic genes to build a better heart. Circulation 2002;106:2043–5.
66. Taegtmeyer H. Tracing cardiac metabolism in vivo: one substrate at a time. J Nucl Med 2010;51 Suppl 1:80S–7S.
67. Taegtmeyer H, Ballal K. No low-fat diet for the failing heart? Circulation 2006;114:2092–3.
68. Taegtmeyer H, McNulty P, Young ME. Adaptation and maladaptation of the heart in diabetes: part I: general concepts. Circulation 2002; 105:1727–33.
69. Young ME, McNulty P, Taegtmeyer H. Adaptation and maladaptation of the heart in diabetes: part II: potential mechanisms. Circulation 2002;105: 1861–70.
70. Taegtmeyer H. Cardiac metabolism as a target for the treatment of heart failure. Circulation 2004;110:894–6.
71. Taegtmeyer H. Glucose for the heart: too much of a good thing? J Am Coll Cardiol 2005;46:49–50.
72. Nikolaidis LA, Sturzu A, Stolarski C, et al. The development of myocardial insulin resistance in conscious dogs with advanced dilated cardiomyopathy. Cardiovasc Res 2004;61:297–306.
73. Gropler RJ, Beanlands RS, Dilsizian V, et al. Imaging myocardial metabolic remodeling. J Nucl Med 2010;51 Suppl 1:88S–101S.
74. Shoup TM, Elmaleh DR, Bonab AA, Fischman AJ. Evaluation of trans-9-^{18}F-fluoro-3,4-methyleneheptadecanoic acid as a PET tracer for myocardial fatty acid imaging. J Nucl Med 2005;46:297–304.
75. vom Dahl J, Herman WH, Hicks RJ, et al. Myocardial glucose uptake in patients with insulin-dependent diabetes mellitus assessed quantitatively by dynamic positron emission tomography. Circulation 1993;88:395–404.
76. Nikolaidis LA, Elahi D, Hentosz T, et al. Recombinant glucagon-like peptide-1 increases myocardial glucose uptake and improves left ventricular performance in conscious dogs with pacing-induced dilated cardiomyopathy. Circulation 2004; 110:955–61.
77. Slart RH, Bax JJ, de Jong RM, et al. Comparison of gated PET with MRI for evaluation of left ventricular function in patients with coronary artery disease. J Nucl Med 2004;45:176–82.
78. Mistry M, Kagan M, Lazewatsky J, et al. Dosimetry in nonhuman primates of [^{18}F]LMI1195, a novel PET tracer for imaging the cardiac sympathetic nervous system. J Nucl Med 2010;51 Suppl 2:1447 (abstr).
79. Tahara N, Tahara A, Nitta Y, et al. Heterogeneous myocardial FDG uptake and the disease activity in cardiac sarcoidosis. J Am Coll Cardiol Img 2010;3:1219–28.
80. Gould KL. Pressure-flow characteristics of coronary stenoses in unsedated dogs at rest and during coronary vasodilation. Circ Res 1978;43: 242–53.
81. Sun Y, Most AS, Ohley W, Gewirtz H. Estimation of instantaneous blood flow through a rigid coronary artery stenosis in anesthetized domestic swine. Cardiovasc Res 1983;17:499–504.
82. Young DF, Cholvin NR, Roth AC. Pressure drop across artificially induced stenosis in the femoral artery of dogs. Circ Res 1975;36:735–43.
83. Botker HE, Goodwin GW, Holden JE, et al. Myocardial glucose uptake measured with fluorodeoxyglucose: a proposed method to account for variable lumped constants. J Nucl Med 1999;40:1186–96.

Key Words: heart failure ■ myocardial blood flow ■ PET imaging.